

# Light-Scattering Study of Poly(hydroxy ester ether) in *N,N*-Dimethylacetamide Solution

X. CAO,<sup>1</sup> D. J. SESSA,<sup>2</sup> W. J. WOLF,<sup>2,\*</sup> J. L. WILLETT<sup>2</sup>

<sup>1</sup> Department of Chemistry, Bradley University, Peoria, Illinois 61625

<sup>2</sup> Plant Polymer Research, USDA,† ARS, MWA, National Center for Agricultural Utilization Research, 1815 N. University Street, Peoria, Illinois 61604

Received 7 December 1999; accepted 19 May 2000

**ABSTRACT:** Static and dynamic light-scattering techniques were used to study biodegradable thermoplastic poly(hydroxy ester ether) in *N,N*-dimethylacetamide (DMAc). A weight-average molecular weight  $M_w = 6.4 \times 10^4$  g/mol, radius of gyration  $R_G = 9.4$  nm, second-virial coefficient  $A_2 = 1.05 \times 10^{-3}$  mol mL/g<sup>2</sup>, translational diffusion coefficient  $D = 1.34 \times 10^{-7}$  cm<sup>2</sup>/s, and hydrodynamic radius  $R_H = 8.3$  nm are reported. In addition, the effect of H<sub>2</sub>O on the polymer chain's conformation and architecture in a DMAc/H<sub>2</sub>O solution is evaluated. Results suggest that H<sub>2</sub>O makes the mixed solvent poorer as well as promotes polymer chain branching via intramolecular transesterification. © 2001 John Wiley & Sons, Inc. *J Appl Polym Sci* 80: 1737–1745, 2001

**Key words:** light scattering; poly(hydroxy ester ether); *N,N*-dimethylacetamide; mixed solvent; chain architecture

## INTRODUCTION

Poly(hydroxy ester ethers) (PHEEs) are a group of hydroxy-functional polyesters synthesized by polymerizing diacids with stoichiometrically equivalent amounts of diglycidyl esters, catalyzed by quaternary ammonium halide.<sup>1–3</sup> High molecular weight, thermoplastic PHEEs can be conveniently prepared by this method. The polymer derived from the diglycidyl ether bisphenol A and

adipic acid [HOOC—(CH<sub>2</sub>)<sub>4</sub>—COOH] is an amorphous material with a glass transition temperature,  $T_g$ , of 45°C. This thermoplastic biodegradable resin, referred to as PHEE, has good barrier and mechanical properties.<sup>3</sup>

In this study, light scattering (LS), both static and dynamic, was used to characterize this PHEE polymer in a *N,N*-dimethylacetamide (DMAc) solution. Parameters such as weight-average molecular weight  $M_w$ , radius of gyration  $R_G$ , second-virial coefficient  $A_2$ , translational diffusion coefficient  $D$ , and hydrodynamic radius  $R_H$  were measured. In addition, the effect of the presence of water, an effective plasticizer for the polymer, was also evaluated.

## EXPERIMENTAL

### Chemicals

PHEE resins (in pellet form) were provided by the Dow Chemical Co. (Midland, MI), synthesized as

Correspondence to: J. L. Willett.

\* Retired.

† Names are necessary to report factually on available data; however, the USDA neither guarantees nor warrants the standard of the product, and the use of the name by USDA implies no approval of the product to the exclusion of others that may also be suitable.

Contract grant sponsors: Agricultural Research Service; Biotechnology Research and Development Corp.; contract grant number: 58-3K95-8-0632.

*Journal of Applied Polymer Science*, Vol. 80, 1737–1745 (2001)  
© 2001 John Wiley & Sons, Inc.

described in the literature. The solvent DMAc, HPLC grade, 99.9%, was purchased from Aldrich (Milwaukee, WI) and was used without any further purification. Reagent-grade water was obtained from a Barnstead (Dubuque, IA) Easypure UV/VF water-filtration system.

### Solution Preparation

PHEE/DMAc stock solutions were prepared by dissolving PHEE resin in DMAc at room temperature under gentle magnetic stirring overnight. Subsequent dilutions were made by adding the solvent to the stock solution to make solutions of desired concentrations (mg/mL). Solutions of PHEE in a mixed solvent of DMAc + H<sub>2</sub>O were made by mixing DMAc and H<sub>2</sub>O to achieve the desired H<sub>2</sub>O content (percent by volume) in the mixed solvent, then by following the general procedure as described above to prepare stock solutions and the subsequent dilutions. Solutions for LS experiments were filtered through Whatman (Clifton, NJ) disposable syringe filters (PTFE filter media with polypropylene housing, 25-mm diameter, 0.2- $\mu$ m pore size) into acetone-rinsed and dried scintillation vials (SVs) for measurement. The samples were allowed to stand for 2 weeks prior to LS measurements.

### Specific Refractive Index Increment ( $dn/dc$ )

This parameter was measured using a Chromatix<sup>TM</sup> KMX-16 laser differential refractometer, with a He—Ne laser ( $\lambda = 632.8$  nm) as a light source. The refractometer was calibrated with aqueous NaCl solutions of seven different concentrations, ranging from 0.5 to 2 g NaCl/100 g H<sub>2</sub>O. The measurements were made at 25°C.

The determination of the differential refractive index is accomplished by measuring the deviation of the He—Ne laser beam passing through a divided cell composed of adjacent solvent and solution compartments. The beam deviation is proportional to the difference in the refractive index ( $\Delta n$ ) between the polymer solution and the respective solvent. To calculate  $\Delta n$ , the beam deviation is multiplied by a calibration constant, determined from the calibration procedure with NaCl<sub>(aq)</sub> as described above. In this study, polymer solutions of five different concentrations, ranging from 2 to 10 mg/mL, were used for the  $\Delta n$  measurements. The slope of the linear least-squares fitting of  $\Delta n$  versus  $c$  yielded  $dn/dc$ .

### Static Light Scattering (SLS)

A DAWN-DSP laser photometer (Wyatt Technology Corp., WTC, Santa Barbara, CA) was used off-line to determine the  $M_w$ ,  $R_G$ , and  $A_2$  of the PHEE/DMAc systems. The LS signals were detected simultaneously at 18 scattering angles,  $\theta$ , ranging from 22.5° to 147°. A He—Ne laser with  $\lambda = 632.8$  nm was used as the light source. The apparatus was operated in the batch mode, using an SV as the scattering cell. All measurements were made at  $25.0 \pm 0.2^\circ\text{C}$ . The operation software was ASTRA<sup>TM</sup> 4.7 for Windows<sup>TM</sup>, provided by WTC. The same software was also used for data analysis. The photometer was calibrated with toluene filtered through a 0.02- $\mu$ m filter (Whatman Anotop<sup>TM</sup>) and normalized with a 10 mg/mL polystyrene/toluene solution ( $M_w = 4000$ ,  $M_w/M_N = 1.04$ ).

The basis for SLS data analysis is the following equation<sup>4</sup>:

$$\frac{R_\theta}{Kc} = M_w P(\theta) - 2A_2 c M_w^2 P^2(\theta) \quad (1)$$

The excess Rayleigh ratio,  $R(\theta)$ , depends on the intensity of the scattered light  $I(\theta)$ .  $K$  is an optical constant,  $K = 4\pi^2 n^2 (dn/dc)^2 \lambda^{-4} N_A^{-1}$ , where  $n$  is the refractive index of the solvent;  $\lambda$ , the wavelength of the incident beam;  $dn/dc$ , the specific refractive index increment of the polymer/solvent system; and  $N_A$ , Avogadro's number.  $P(\theta)$  is the form factor which depends on the polymer size ( $R_G$ ), shape, and structure:

$$P(\theta) = 1 - \frac{(R_G^2 q^2)}{3} + O(q^4), \quad (2)$$

where  $q = (4\pi n/\lambda) \sin(\theta/2)^\ddagger$  is the scattering vector.

From the limits of  $R(\theta)$  as  $\theta \rightarrow 0$ ,  $c \rightarrow 0$ , parameters  $M_w$ ,  $R_G$ , and  $A_2$  can be obtained. This can be achieved by either the Zimm plot of  $Kc/R(\theta)$  versus  $\sin^2(\theta/2)$  or with the Berry plot of  $[Kc/R(\theta)]^{1/2}$  versus  $\sin^2(\theta/2)$ . In this study, the Berry method was used throughout the analysis, since, in some of our cases, the Zimm plot gave erroneous results such as negative  $R_G$  values. The SLS

<sup>‡</sup> The refractive index for a mixed solvent,  $n_{ms}$ , was calculated using the Lorenz–Lorentz equation,<sup>5</sup>  $(n_{ms}^2 - 1)/(n_{ms}^2 + 2) = \phi_1 [(n_1^2 - 1)/(n_1^2 + 2)] + \phi_2 [(n_2^2 - 1)/(n_2^2 + 2)]$ , where  $\phi_1$ ,  $\phi_2$ , and  $n_1$ ,  $n_2$  are the volume fractions and refractive indexes of solvent 1 and solvent 2, respectively.

apparatus, the operation system, and the data analysis were verified by measuring a polystyrene molecular weight standard with a narrow distribution (Polysciences, Inc., Warrington, PA,  $M_w = 400,000$ ,  $M_w/M_n = 1.06$ ) in toluene and comparing the measured values with the values supplied by the manufacturer and the values reported in the literature. The results proved to be satisfactory:  $M_w$  (measured) =  $4.08 \pm 0.08 \times 10^5$  g/mol.

### Dynamic Light Scattering (DLS)

DLS measurements were performed with a Brookhaven Instruments Corp. (BIC, Holtsville, NY) BI-9000AT autocorrelator and a variable-scattering angle BIC BI-200SM goniometer with a stepping motor controller, using the  $\lambda = 514.5$ -nm line of an argon laser (Lexel Laser, Inc., Fremont, CA) to illuminate the sample cell, an SV. The sample cell was placed in a thermostatted glass vat with an optically flat window, filled with *cis-trans*-decahydronaphthalene (trade name Decalin) as the index matching liquid to match the refractive index of the SV and the vat. All experiments were carried out at  $25.0 \pm 0.1^\circ\text{C}$ . The scattered intensity at the scattering angle  $\theta$ ,  $I(\theta)$ , was determined using standard photon counting methods. With this instrument, it was possible to cover an angular range of  $\theta = 30^\circ - 150^\circ$ , which corresponds to a range of  $0.9 - 3 \times 10^7 \text{ m}^{-1}$  for the scattering vector  $q$ . Intensity autocorrelation functions,  $G_2(t)$ , covering the decay of the intensity fluctuations over six decades of time were measured.

The decay of  $G_2(t)$  provides a measure of the diffusion coefficient  $D$  of the macromolecules in the solution.<sup>6</sup> If there is only one size of the macromolecule in a dilute solution, then

$$G_2(t) = B + A \exp(-2\Gamma t), \quad (3)$$

where  $A$  denotes the dynamic amplitude, and  $B$ , the baseline of the measured correlation function (related to the total intensity scattered at the scattering vector  $q$ ).  $\Gamma$  is the decay rate. For the motion of particles in solution that is purely diffusive,  $\Gamma$  is related to the diffusion coefficient  $D$  via the following equation:

$$\Gamma = Dq^2 \quad (4)$$

The hydrodynamic radius  $R_H$  of the macromolecule can then be derived from  $D$  by using the Stokes–Einstein equation:

$$R_H = \frac{k_B T}{6\pi\eta D} \quad (5)$$

where  $k_B$  is the Boltzmann constant;  $T$ , the absolute temperature; and  $\eta$ , the viscosity of the solvent.<sup>#</sup>

In a polydisperse solution, there may be many different species, each diffusing with its own characteristic diffusion coefficient. In this case, it is possible to obtain the distribution  $A(D)$  of species with the diffusion coefficient  $D$  from the normalized electric field autocorrelation function,  $g_1(t)$ :

$$g_1(t) = \left[ \frac{(G_2(t) - B)}{A} \right]^{1/2} \quad (6)$$

$$g_1(t) = \int A(D) \exp(-Dq^2 t) dD \quad (7)$$

The determination of  $A(D)$  from eq. (7) can be realized by Laplace inversion techniques. In this study,  $A(D)$  was obtained from the measured correlation functions by using the REPES program which employs the Laplace inversion.<sup>7–10</sup>

The alignment of the DLS system was checked by measuring the  $I(\theta)$  of filtered toluene in the range of  $\theta = 15^\circ - 155^\circ$ , then plotting  $I(\theta)\sin(\theta)$  versus  $\theta$ . The alignment proved to be satisfactory: % error [of  $I(\theta)\sin(\theta)$  normalized to average]  $\leq 1.3\%$ . The operation of the system and the data analysis were verified by measuring the size of the polystyrene nanospheres suspended in water and then comparing the calculated  $R_H$  value to that provided by the manufacturer. The agreement was good:  $R_H$  (manufacturer) =  $48 \pm 1.6$  nm;  $R_H$  (measured) =  $48.2 \pm 0.3$  nm.

## RESULTS AND DISCUSSION

### Specific Refractive Index Increment $dn/dc$ Measurements

The  $dn/dc$  value was measured using a series of PHEE solutions in the concentration range  $2 < c < 10$  mg/mL. At least eight readings were taken at each concentration, and a standard deviation

<sup>#</sup> The viscosity for the mixed solvent,  $\eta_{ms}$ , is calculated based on the following equation:  $\eta_{ms} = \phi_1 \eta_1 + \phi_2 \eta_2$ , where  $\eta_1$  and  $\eta_2$  are the viscosities of solvent 1 and solvent 2, respectively.

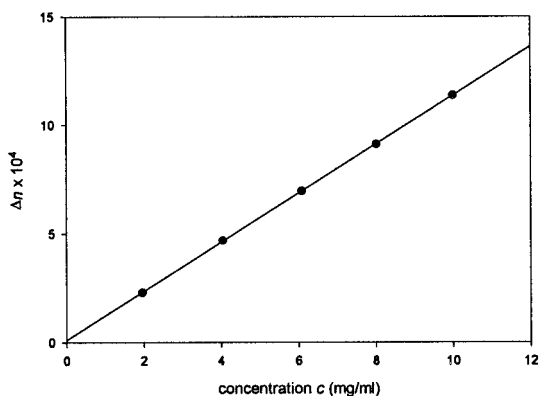


**Figure 1** Determination of the specific refractive index increment  $dn/dc$  for PHEE/DMAc at 25°C. The error bars for the data points were smaller than the size of the symbols used. The standard deviation for  $dn/dc$ :  $dn/dc = 0.113 \pm 0.0003$  mL/g, was obtained by linear least-squares fitting of the data.

was calculated based on the mean value of these readings. A  $\Delta n$  value for each concentration was then obtained from the mean value of the readings for the concentration and the calibration constant of the apparatus, determined as described in the Experimental section. Figure 1 shows the result of  $\Delta n$  versus  $c$  measurements for the PHEE/DMAc solutions. The straight line shows the least-squares fitting. The slope of the fitting gives  $dn/dc$ . The value,  $dn/dc = 0.113 \pm 0.0003$  mL/g, was obtained for PHEE/DMAc at 25°C. This  $dn/dc$  value is in the typical range for polymer solutions.<sup>4</sup>

#### Effect of Solvent on $dn/dc$

The H<sub>2</sub>O content of the solution had a peculiar effect on the  $dn/dc$  value, as shown in Figure 2. Investigation on PHEE solutions of DMAc with different H<sub>2</sub>O content showed that  $dn/dc$  decreases as the H<sub>2</sub>O content increases from 0 to 4%, reaches a minimum at ~4% H<sub>2</sub>O content, then increases as the H<sub>2</sub>O content increases. It is speculated that there is certain degree of complex formation between PHEE and DMAc. The addition of H<sub>2</sub>O breaks down this complex structure. At 4% H<sub>2</sub>O content, the complex structure is completely destroyed. The  $dn/dc$  value then increases monotonically with the increasing H<sub>2</sub>O content beyond 4% H<sub>2</sub>O, since the refractive index of H<sub>2</sub>O is smaller than that of DMAc:  $n_{\text{H}_2\text{O}} = 1.333$  versus  $n_{\text{DMAc}} = 1.438$ .

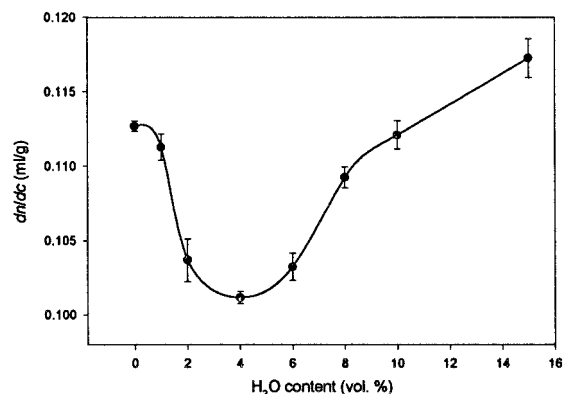


**Figure 2**  $dn/dc$  values of PHEE with different H<sub>2</sub>O contents. Each  $dn/dc$  value and its standard deviation were determined as described in the text and in Figure 1. The curve is drawn to guide the eye.

#### SLS Measurements

SLS measurements were carried out on the WTC DAWN-DSP photometer; all measurements were made at  $25.0 \pm 0.2^\circ\text{C}$ . The Berry plot, based on eq. (1), was used for data analysis. The  $dn/dc$  values used in the calculation were measured as described above. In general, five concentrations ranging from 2 to 10 mg/mL were used, and scattering intensities at 18 scattering angles were collected and used in the calculation. Values at low  $\theta$  were less certain in some cases, as expected. However, the calculation results were not significantly changed if the scattering values at low  $\theta$  were eliminated from the data analysis. To be consistent, all scattering angles were used in the calculation throughout the data analysis for different systems.

Figure 3 shows the Berry plot for the PHEE/

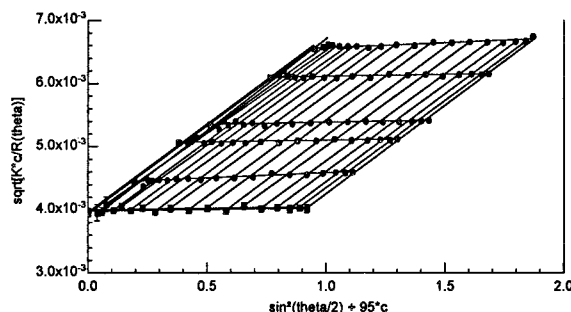


**Figure 3** Berry plot for PHEE in DMAc. Concentrations of the five solutions:  $c_1 = 2.03$  mg/mL;  $c_2 = 4.01$  mg/mL;  $c_3 = 5.39$  mg/mL;  $c_4 = 8.04$  mg/mL;  $c_5 = 10.00$  mg/mL. The range of the scattering angles measured was  $22.5^\circ$ – $147^\circ$ .



**Table I** Molecular Parameters of PHEE in DMAc with Different H<sub>2</sub>O Contents, Measured by SLS at 25°C

H <sub>2</sub> O Content (vol %)	$M_w \times 10^{-4}$ (g/mol)	$R_G$ (nm)	$A_2 \times 10^4$ (mol mL g <sup>-2</sup> )
0	6.4 ± 0.09	9.4 ± 3.8	10.46 ± 0.36
1.0	6.4 ± 0.05	16.7 ± 1.1	9.68 ± 0.16
2.0	7.3 ± 0.08	15.4 ± 2.0	8.40 ± 0.21
4.0	7.4 ± 0.09	17.8 ± 1.9	7.27 ± 0.21
6.0	7.6 ± 0.07	22.0 ± 1.3	7.00 ± 0.16
8.0	6.4 ± 0.03	14.6 ± 1.1	6.67 ± 0.12
10.0	6.2 ± 0.08	18.3 ± 1.6	5.51 ± 0.27

DMAc solution. The results are  $M_w = 6.4 \pm 0.09 \times 10^4$  g/mol,  $R_G = 9.4 \pm 3.8$  nm, and  $A_2 = 1.05 \pm 0.036 \times 10^{-3}$  mol mL g<sup>-2</sup>. Within experimental error, the  $M_w$  value obtained here is identical to that measured by gel permeation chromatography (GPC) at Dow Chemical:  $M_w = 6.5 \times 10^4$  g/mol.<sup>||</sup> The large, positive value of  $A_2$  indicates that DMAc is a good solvent for PHEE at 25°C. The relatively large uncertainty of  $R_G$  (~40%) is probably due to the fact that the size of the macromolecule measured is at the lower limit of the instrument (~10 nm). However, it is necessary to point out here that the ASTRA software package (by WTC) offers different polynomial degrees for concentration and angle fits of the scattering data. The fitting results,  $R_G$  values in particular, are dependent on the fitting degrees used. (For example,  $R_G = 27.6 \pm 3.5$  nm is obtained when the first-degree angle fit and second-degree concentration fit are used in the Berry plot to analyze the same set of data as shown in Fig. 3.) To be consistent, first-degree concentration and angle fits were used in the Berry plot for all SLS data analysis.

Table I summarizes the measured SLS results for PHEE in DMAc with different H<sub>2</sub>O contents. Of the three parameters measured,  $M_w$  seems to have two different groups of values:  $M_w \sim 6.4 \times 10^4$  g/mol at H<sub>2</sub>O contents of 0, 1.0, 8.0, and 10.0%, and  $M_w \sim 7.4 \times 10^4$  g/mol at H<sub>2</sub>O contents of 2.0, 4.0, and 6.0%. The reason for this variation is not clear to us at this point. The  $R_G$  values, except for two solutions at H<sub>2</sub>O contents of 0 and 6.0%, remained relatively unchanged, with a mean value at ~17 nm. Only  $A_2$  had a definitive

trend with the change in H<sub>2</sub>O content. It decreased monotonically as the H<sub>2</sub>O content increased, from  $1.05 \times 10^{-3}$  at 0% H<sub>2</sub>O content to  $5.5 \times 10^{-4}$  mol mL g<sup>-2</sup> at 10.0% H<sub>2</sub>O content, a 50% decrease. This clearly indicates that the addition of H<sub>2</sub>O to DMAc makes it a poorer solvent for the polymer.<sup>11</sup>

### Overlap Concentration

The transition from dilute to semidilute for a polymer solution occurs at a concentration designated as  $c^*$ , at which point the macromolecules will fill the available volume. de Gennes<sup>12</sup> introduced the concept of “overlap concentration” for  $c^*$ , since, in the semidilute region, the individual chains overlap to form many contacts and become entangled. For dilute solutions,  $c < c^*$ , the macromolecules are so far apart from each other that any interactions between macromolecules are virtually negligible and have little impact on any physical properties of the solution. For semidilute solutions at  $c > c^*$ , a drastic change in the solution properties is expected and generally observed. The value of  $c^*$  depends on factors such as the definition of a polymer chain’s dimension and conformation. For flexible linear chains, the following conventions are often used<sup>13</sup>:

$$c_{R_G}^* = \frac{M_w/N_A}{\frac{4\pi}{3} R_G^3} \quad (8)$$

$$c_{R_H}^* = \frac{M_w/N_A}{\frac{4\pi}{3} R_H^3} \quad (9)$$

$$c_{A_2}^* = (A_2 M_w)^{-1} \quad (10)$$

Using the average values from SLS measurements for the PHEE solutions,  $M_w = 6.8 \times 10^4$  g/mol,  $R_G = 16.3$  nm,  $A_2 = 1.05 \times 10^{-3}$  mol mL g<sup>-2</sup> (PHEE/DMAc), and  $R_H = 10.1$  nm (see the following section),  $c^*$  was calculated from eqs. (8), (9), and (10):  $c_{R_G}^* = 6$  mg/mL,  $c_{R_H}^* = 26$  mg/mL, and  $c_{A_2}^* = 14$  mg/mL.

The differences among  $c_{R_G}^*$ ,  $c_{R_H}^*$ , and  $c_{A_2}^*$  values are not surprising. Since  $c^*$  cannot be uniquely defined, various  $c^*$  definitions can differ in value by a factor of up to 10. Here,  $c^*$  is only used as a guideline to determine the borderline between dilute and semidilute regions. The highest con-

<sup>||</sup> Dow Chemical Application Note.

centration used here was 10 mg/mL; the lowest was 2 mg/mL, and the experimental results were extrapolated to  $c \rightarrow 0$  to obtain parameters such as  $M_w$ ,  $R$ , etc. Therefore, it is safe to assume that the solutions studied here are dilute solutions; it is also valid to use the well-established theoretical procedures for the dilute region for data interpretation, and the results obtained reflect the physical properties of the macromolecules.

### DLS Measurements

The same samples used in the SLS studies were used for the DLS measurements. Figure 4(A) shows an example of the experimentally measured autocorrelation function for PHEE/DMAc. The distribution  $A(D)$  versus  $D$  is calculated by the REPES program according to eqs. (6) and (7).  $R_H$  is then obtained via eq. (5), and the resulting distribution profile of  $A(R_H)$  versus  $R_H$  is shown in Figure 4(B). It is evident that the autocorrelation function in Figure 4(A) does not show distinguish-

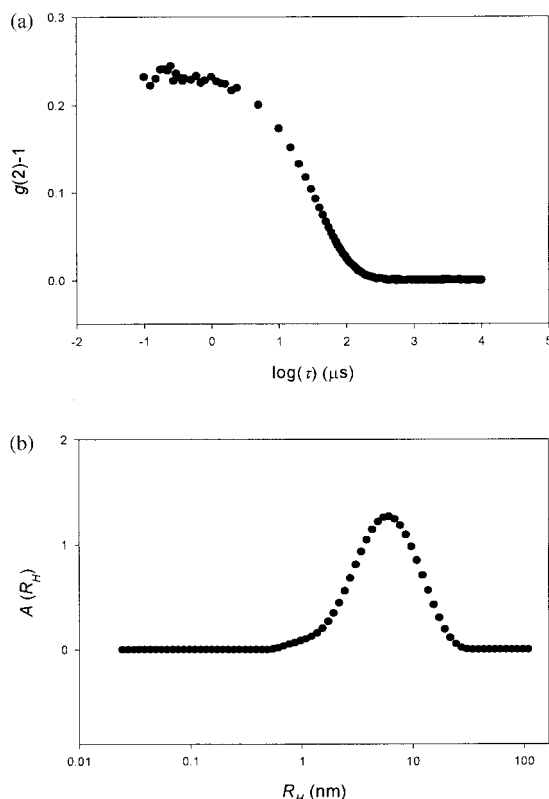


**Figure 4** (a) Intensity autocorrelation function for PHEE/DMAc,  $c = 2.0$  mg/mL, measured by DLS at  $\theta = 90^\circ$ ,  $25^\circ\text{C}$ . (b) Distribution of hydrodynamic radius  $R_H$  obtained by the REPES analysis from the correlation function shown in (a).

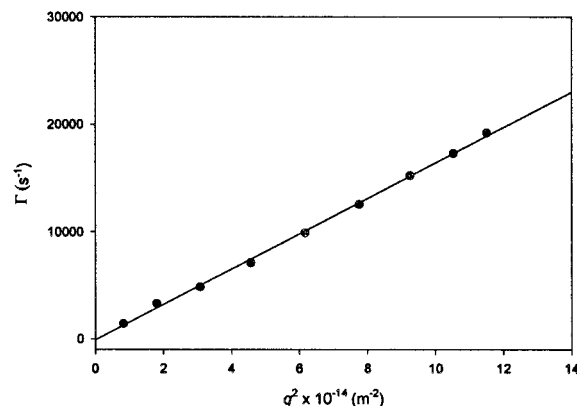


**Figure 5** The  $q$ -dependence of the decay rate,  $\Gamma$ , obtained by the REPES analysis for PHEE in DMAc. The straight line represents a least-squares fitting, and the slope of the fitting gives the diffusion coefficient  $D$ .

ably different diffusion modes. This is also demonstrated by the Laplace inversion of the correlation function: the resulting distribution [as shown in Figure 4(b)] shows a broad singular distribution with no apparent aggregates present. This indicates that the PHEE polymer used in this study has a broad molecular weight distribution, which is in good agreement with the manufacturer's GPC measurements.<sup>§</sup>

DLS measurements for each solution were made in the  $\theta$  range of  $30^\circ$ – $150^\circ$ , at  $15^\circ$  increments. The value of the decay rate  $\Gamma_{(\theta)}$ , which represents the average value of the broad singular distribution, was then obtained through eqs. (3), (4), (6), and (7). Figure 5 shows as an example the  $q$ -dependence of  $\Gamma_{(\theta)}$  for PHEE in DMAc. The excellent linear relationship between  $\Gamma_{(\theta)}$  and  $q^2$  implies that the motion is indeed purely diffusive. The diffusion coefficient  $D$  is then obtained as the slope of the  $\Gamma_{(\theta)}$  versus  $q^2$  fit. Subsequently, the  $D$  value for each solution was obtained by this method.

As in SLS, for each PHEE/DMAc +  $\text{H}_2\text{O}$  system, five different concentrations ranging from 2 to 10 mg/mL were used in the DLS measurements, and Figure 6 shows the typical concentration dependence of  $D$ . It is evident that  $D$  increases as  $c$  increases. It is known that<sup>14</sup>

$$D_{(c)} \sim D_0(1 + k_d c) \quad (11)$$

$$k_d = 2A_2M_w - \frac{C_D N_A R_H^3}{M_w} \quad (12)$$

<sup>§</sup> Dow Chemical Application Note.

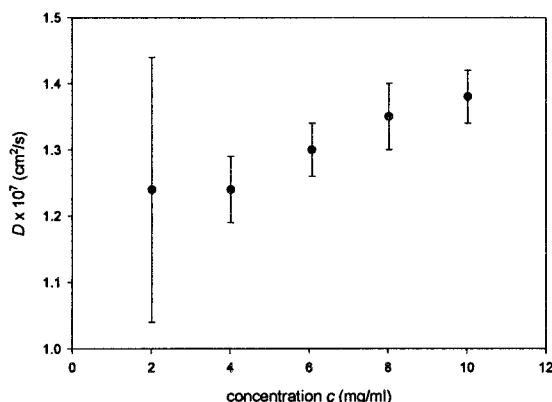


**Figure 6** Concentration dependence of diffusion coefficient  $D$ . The  $D$  value and the error bar at each concentration were determined as described in the text and in Figure 5. Solution used: PHEE in DMAc with 4.0%  $\text{H}_2\text{O}$  content.  $25^\circ\text{C}$ .

where  $D_0$  is the diffusion coefficient at  $c \rightarrow 0$  and  $C_D$  is a positive constant. A linear fitting of  $D(c)$  versus  $c$  according to eq. (11) would yield  $D_0$  and  $k_d$  values. Table II shows the fitting results.

The monotonic decrease of  $k_d$  with increasing  $\text{H}_2\text{O}$  content can be explained by eq. (12). It is known from SLS studies, as described in the previous section and in Table I, that  $A_2$  decreases with increasing  $\text{H}_2\text{O}$  content and  $M_w$  remains relatively unchanged. Therefore, the thermodynamic term ( $2A_2M_w$ ) for  $k_d$  decreases with increasing  $\text{H}_2\text{O}$  content. The hydrodynamic term ( $C_D N_A R_H^3 / M_w$ ) increases with increasing  $\text{H}_2\text{O}$  content, because of increasing  $R_H$  (decreasing  $D_0$ , as shown in Table II). The combined result is that  $k_d$  decreases with increasing  $\text{H}_2\text{O}$  content. As a matter of fact, there are studies using the  $k_d$  values to estimate the Flory  $\Theta$ -temperature and  $\Theta$ -solvent.<sup>15</sup> This condition did not materialize in this study, however, because the lowest  $A_2$  at

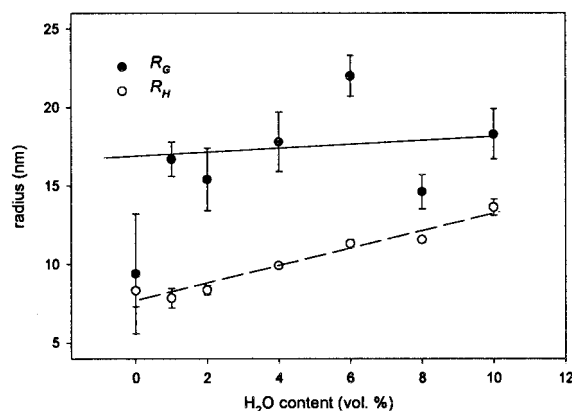


**Figure 7** Hydrodynamic radius  $R_H$  and radius of gyration  $R_G$  of PHEE in DMAc at different  $\text{H}_2\text{O}$  contents. The lines were drawn to guide the eye; the first  $R_G$  point was not included in drawing the line because of its large uncertainty. The numerical values of  $R_H$  and  $R_G$  can be found in Tables I and II.

10.0%  $\text{H}_2\text{O}$  content is still  $5.5 \times 10^{-4} \text{ mol mL g}^{-2}$ , close but not yet to 0, suggesting that this particular mixed solvent at  $25^\circ\text{C}$  has not quite yet reached the  $\Theta$ -conditions.

Figure 7 shows the hydrodynamic radius  $R_H$ , as determined from the diffusion coefficient  $D_0$  via eq. (5) of PHEE in DMAc with different  $\text{H}_2\text{O}$  contents, as well as  $R_G$ . The increase of  $R_H$  with increasing  $\text{H}_2\text{O}$  content is apparent, while  $R_G$  remains relatively unchanged. Figure 8 shows the distribution profiles of PHEE in DMAc with four different  $\text{H}_2\text{O}$  contents. The shape of the distribution does not change significantly as the  $\text{H}_2\text{O}$  content changes. Instead, the whole distribution shifts toward larger  $R_H$  as the  $\text{H}_2\text{O}$  content increases. In other words, the increase in  $R_H$  is not caused by the formation of some distinguishably larger aggregates, because no separate slow

**Table II** Dynamic Parameters Obtained by DLS on PHEE in DMAc with Different  $\text{H}_2\text{O}$  Contents According to Eq. (11)

$\text{H}_2\text{O}$ Content (vol %)	$D_0 \times 10^7 \text{ (cm}^2/\text{s)}$	$k_d \times 10^2 \text{ (mL/mg)}$	$R_H \text{ (nm)}$	$\rho \text{ (} R_G/R_H \text{)}$
0	$1.34 \pm 0.17$	$6.3 \pm 2.3$	$8.3 \pm 1.0$	$1.13 \pm 0.68$
1.0	$1.43 \pm 0.11$	$4.6 \pm 1.7$	$7.8 \pm 0.6$	$2.13 \pm 0.34$
2.0	$1.35 \pm 0.05$	$2.2 \pm 0.7$	$8.4 \pm 0.3$	$1.84 \pm 0.31$
4.0	$1.15 \pm 0.02$	$1.9 \pm 0.3$	$9.9 \pm 0.1$	$1.79 \pm 0.22$
6.0	$1.02 \pm 0.02$	$1.9 \pm 0.4$	$11.3 \pm 0.2$	$1.94 \pm 0.16$
8.0	$1.01 \pm 0.02$	$1.0 \pm 0.3$	$11.6 \pm 0.001$	$1.26 \pm 0.10$
10.0	$0.867 \pm 0.033$	$0.92 \pm 0.5$	$13.6 \pm 0.5$	$1.34 \pm 0.18$

$D_0$  is the intercept at  $c \rightarrow 0$  of the linear least-squares fitting and  $k_d$  is the slope.  $R_H$  is calculated from  $D_0$  according to eq. (5).

modes representing large aggregates were seen in the distribution profile.

The notion that no large aggregates were formed with the addition of H<sub>2</sub>O was further supported by the SLS results, which demonstrated that  $M_W$  and  $R_G$  remain relatively unchanged with increasing H<sub>2</sub>O content, as described in the previous section. The question that has to be answered here is why  $R_H$  increases while  $R_G$  and  $M_W$  remain unchanged. There are principally two possibilities: (I) a change in PHEE's polydispersity and/or (II) a change of the polymer chain conformation and/or architecture. Figure 8 shows that the distribution profile does not change drastically with the addition of H<sub>2</sub>O; therefore, polymer polydispersity does not play a major role here. A parameter that has strong chain conformation/architecture dependence is the so-called  $\rho$  parameter that can be obtained from a combination of dimensions measured by SLS and DLS, that is,  $R_G$  and  $R_H$ :  $\rho = R_G/R_H$ . The  $\rho$  parameter has been calculated for different chain conformation, architecture, and polydispersity<sup>16</sup>:  $\rho > 2$  for a rigid rod,  $\rho \sim 2$  for a polydisperse random coil in a good solvent and decreases to  $\rho \sim 1.7$  in  $\Theta$ -solvent,  $\rho \sim 1.0$ – $1.3$  for branched chains under  $\Theta$ -conditions, and  $\rho \sim 0.78$  for uniform spheres. The  $\rho$  parameters for PHEE in DMAc with different H<sub>2</sub>O contents are listed in Table II.

Except for the system of PHEE in pure DMAc where the  $R_G$  value is somewhat problematic ( $\sim 40\%$  uncertainty), as discussed in the previous section,  $\rho$  for PHEE in DMAc decreases as the H<sub>2</sub>O content increases, as shown in Figure 9. At low H<sub>2</sub>O contents (1.0–6.0%),  $\rho > 1.7$ , indicating

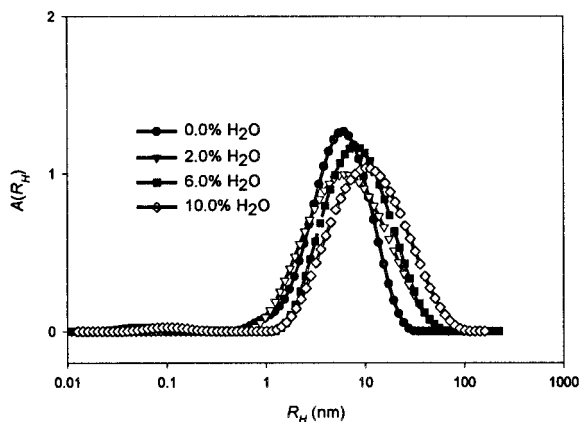


**Figure 8** Distribution profiles of  $R_H$  for PHEE in DMAc with different H<sub>2</sub>O contents, determined as described in the text and Figure 4.

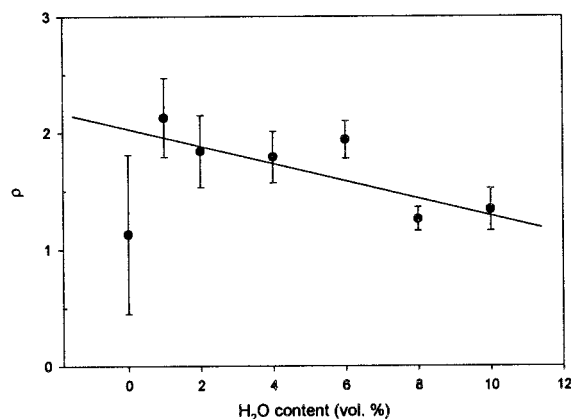


**Figure 9**  $\rho$  ( $R_G/R_H$ ) of PHEE in DMAc at different H<sub>2</sub>O contents. The line is drawn to show that  $\rho$  decreases with increasing H<sub>2</sub>O content. The first  $\rho$  point was not included in drawing the line because of its large uncertainty. The numerical values of  $\rho$  can be found in Table II.

that the solvent is indeed a good solvent, and PHEE assumes an expanded random coil conformation in the solution. As the H<sub>2</sub>O content increases, the solvent becomes poorer, and at 8–10% H<sub>2</sub>O contents, the system has a  $\rho$  parameter equivalent to a star polymer ( $f = 4$ ,  $f$  = number of rays per star, functionality of the star center,  $f = 1$  for linear polymer) under  $\Theta$ -conditions, for example,  $\rho = 1.3$ . In other words, the addition of H<sub>2</sub>O to the PHEE/DMAc system does two things: (I) it makes the solvent poorer for the polymer, and (II) at H<sub>2</sub>O contents  $\geq 8.0\%$ , it causes the polymer to undergo a structural rearrangement to assume an architecture similar to a star polymer. Because  $M_W$  as measured by SLS does not change, the structural rearrangement must be predominantly intramolecular in nature. Since PHEE has a tendency to participate in an intramolecular transesterification reaction,<sup>2</sup> it is therefore speculated that the addition of H<sub>2</sub>O promotes this intramolecular transesterification, thus producing branched polymer chains while  $M_W$  values and the distribution profiles remain unchanged. The dense packing of branched chains prevents more and more the draining of the solvent; therefore,  $R_H$  increases strongly as the degree of branching increases while  $R_G$  remains relatively unchanged—hence, the decrease of  $\rho$ .

## CONCLUSIONS

SLS and DLS were used to characterize PHEE in DMAc and to study the effect of H<sub>2</sub>O on the sys-



tem. The results showed that DMAc at 25°C is a good solvent for the polymer, and the addition of H<sub>2</sub>O makes the mixed solvent poorer. Moreover, the results showed that  $M_w$ ,  $R_G$ , and the distribution profile of the polymer remain unchanged, while  $R_H$  values increase with increasing H<sub>2</sub>O content. That H<sub>2</sub>O promotes PHEE's intramolecular structural rearrangement is the mechanism proposed to explain the above observations.

Comments on the manuscript by Dr. E. Bagley of BRDC are gratefully acknowledged by the authors. M. Mang and S. Kram of Dow Chemical provided GPC data for PHEE. One of the authors (X. C.) thanks R. Myers and L. Nilsson of WTC for their help on the DAWN-DSP. This research was conducted under CRADA number 58-3K95-8-0632 between the Agricultural Research Service and the Biotechnology Research and Development Corp.

## REFERENCES

1. Mang, M. N.; White, J. E. U.S. Patent 5,171,820, 1992 (to Dow Chemical Co.).
2. Mang, M. N.; White, J. E.; Haag, A. P.; Kram, S. L.; Brown, C. N. *Polym Prepr* 1995, 36, 180–181.
3. Mang, M. N.; White, J. E.; Kram, S. L.; Rick, D. L.; Bailey, R. E.; Swanson, P. E. *Polym Mater Sci Eng* 1997, 76, 412–413.
4. Huglin, M. B. *Light Scattering from Polymer Solutions*; Academic: London, New York, 1972.
5. Chu, B.; Wu, D.-Q. *Macromolecules* 1987, 20, 1606–1619.
6. Berne, B. J.; Pecora, R. *Dynamic Light Scattering*; Wiley: New York, 1976.
7. Provencher, S. W.; Hendrix, J.; Maeyer, L. D.; Paulussen, N. *J Chem Phys* 1978, 69, 4273–4276.
8. Jakes, J. *Collect Czech Chem Commun* 1995, 60, 1781–1797.
9. Jakes, J. *Czech J Phys* 1988, 38, 1305–1316.
10. Stepanek, P.; Johnsen, R. M. *Collect Czech Chem Commun* 1995, 60, 1941–1949.
11. Flory, P. J. *Principles of Polymer Chemistry*; Cornell University: Ithaca, London, 1953.
12. de Gennes, P. G. *Scaling Concepts in Polymer Physics*; Cornell University: Ithaca, London, 1979.
13. Freed, K. F. *Renormalization Group Theory of Macromolecules*; Wiley: New York, 1987.
14. Yamakawa, H. *Modern Theory of Polymer Solution*; Harper and Row: New York, 1971.
15. Lau, A. C. W.; Wu, C. *Macromolecules* 1999, 32, 581–584.
16. Burchard, W.; Schmidt, M.; Stockmayer, W. H. *Macromolecules* 1980, 13, 1265–1272.